Summary: A novel polystyrene-encapsulated laponite composite system has been developed via a miniemulsion polymerization approach. The encapsulation mechanism and process parameters have been examined in detail using light-scattering, sedimentation analysis, wide-angle X-ray diffraction (WXRD), and transmission electron microscopy (TEM). The laponite was encapsulated through a miniemulsion polymerization process in which laponite was predispersed in the monomer phase. The stability of both the miniemulsion and the latex depends on initiation loci, premixing procedures, intensity and time of ultrasonification and the surfactants and co-stabilizer used. Hydrophobicity of the laponite clay played a vital role in both the encapsulation of the clay and the stability of the latex. A quaternary ammonium salt, cetyltrimethylammonium bromide (CTAB), was mixed with the clay in the monomer phase prior to emulsification. As a result, the clay particles were hydrophobically modified and were intercalated. The hydrophobicity not only favored the clay dispersion in the oil droplets but also aided the entry of the monomer into the clay's intergalleries during polymerization. Meanwhile, CTAB helped stabilize the system when it was used in conjunction with the nonionic surfactant polyoxyethylene (40) isooctylphenyl ether (TX-405). In this way, the laponite is effectively encapsulated within a polystyrene shell in a stable latex form. More importantly, the polymerization initiated in the intergalleries of the clay effectively expands the clay's platelet array to form an exfoliated structure.

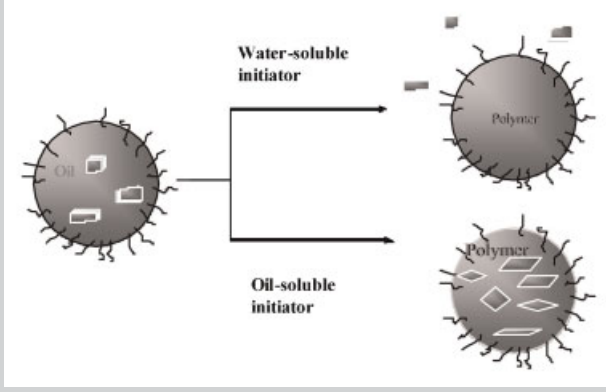

Synthesis and Characterization of Polystyrene-Encapsulated Laponite Composites via Miniemulsion Polymerization

Qunhui Sun,[1] *Yulin Deng,**[1] *Zhong Lin Wang*[2]

[1] School of Chemical Engineering, Georgia Institute of Technology, 500 10th Street N.W., Atlanta, Georgia 30332-0620, USA
Fax: 1-404-894-4778; E-mail: Yulin.Deng@ipst.edu
[2] School of Materials Science and Engineering, Georgia Institute of Technology, 771 Feyst Drive, N.W., Atlanta, Georgia 30332-0245, USA

Received: July 20, 2003; Revised: September 12, 2003; Accepted: September 22, 2003; DOI: 10.1002/mame.200300219

Keywords: encapsulation; exfoliation; latices; miniemulsion polymerization; nanocomposites

Introduction

Polymer-nanoclay composite materials have attracted considerable interest among materials scientists recently[1] because of the pioneering work carried out by a research group in the Toyota Central Research Laboratories. The group applied a nylon-montmorillonite clay nanocomposite as an under-the-hood structural part in the engine compartment of an automobile with significantly improved tensile strength, modulus, and heating distortion temperature at no compromise of impact strength of the material.[2] Later on, the researches were extended to other polymer-layered systems, and a range of properties were exploited, such as barrier properties,[3] temperature responsibility,[4] anti-corrosivity,[5] and low thermal coefficient of expansion of materials.[6] These properties are unattainable without using the nanoclay.

The nanoscale phyllosilicate platelets are derived from natural clay minerals (montmorillonite, hectorite, vermiculite, etc.), which are made of two-dimensional 1 nm layers of an aluminate sheet sandwiched between two silicate sheets.[4,7] These layers are stacked together by weak ionic

 DOI: 10.1002/mame.200300219

and van der Waals forces. Under certain conditions, the layers can be partially or completely separated.[8] The polymer/layered phyllosilicate nanocomposite was developed based on evenly dispersing the clay into a polymer matrix by simple mechanical mixing, melt or bulk polymerization, solution polymerization, and emulsion or suspension polymerization approaches.[9] Among the approaches mentioned above, the product in aqueous form has unique advantages, because of the ease of manipulation, low cost, and absence of environmental concerns. A direct application for the improvement of paper coating properties can be taken as an example. Conventional paper coating has involved the simple mixing of polymer binder in a latex form with microparticulates, such as bentonite, kaolin, or calcium carbonate. This means that comprehensive properties of the coating have been restricted. If, however, the polymer/layered phyllosilicate nanocomposites could be used, it would be possible to improve the scratch strength, smoothness, gloss, and printing quality of the coatings. This is because the greatest property enhancements occur if fillers are on the nanometer scale and are evenly dispersed throughout the polymer matrix. Thus, research to develop this kind of material not only has theoretical significance, but also points toward a novel way to develop new materials. Furthermore, the extension of this research can be applied to other water-based products, such as paints, toners,[10] coatings and adhesives.

Huang et al.[9] prepared a polymer/clay nanocomposite by suspension polymerization of MMA with montmorillonite. However, the product obtained was not in a thermodynamically stable water dispersion form. The nanocomposite they prepared through emulsion polymerization was a simple process of mixing clay with an as-prepared emulsion latex of PMMA. No substantial encapsulation was observed. Kim and co-workers[11] synthesized a styrene-acrylonitrile (SAN) copolymer-clay nanocomposite using a conventional emulsion polymerization and observed typical electrorheological (ER) behavior from the ER fluid composed of intercalated particles and silicon oil. However, the product they obtained was in a coagulated form. A more recent example reported by Putlitz et al.[12] used Optigel SH, a clay constituting units of pancake-like single clay layers with a thickness of 1.25 nm and a diameter of approximately 28 nm. The clay was mixed with a miniemulsion latex to prepare so-called ''armored latexes.'' The process was a templating process which forms a hollow inorganic shell with an Optigel SH clay sheet comprising the outer layer of a cationic miniemulsion latex particle. Nevertheless, there was no substantial encapsulation of polymer on nanoclay as described above. The investigations on encapsulation of inorganic particles, such as titanium dioxide (TiO_2),[13] $CaCO_3$,[14] and carbon black[15] are enormous. However, these particles are not intercalatable or exfoliable so further applications are restricted.

In rationalizing the process, several factors had been taken into account. First of all, suspension polymerization can be excluded from the list of considerations, in terms of the final product form. The conventional emulsion polymerization is also not available in terms of the contradiction between the nucleation mechanism of this approach and the location of clay to be encapsulated, even though it has been a powerful tool in manipulating a wide range of latex products. Our preliminary experiments also verified this judgment. It is natural to be concerned with the loci of the clay before and after polymerization in rationalizing the approach, as depicted in Scheme 1. If a phyllosilicate clay particle must be kept separate within a droplet, it should withstand coalescence and coagulation caused by the collision of droplets under high shear. There should be no transfer of oligomeric radicals from the swollen micelles in the aqueous phase into the oil phase, where the clay exists, for this will unavoidably cause coagulation, if the nucleation mechanism in a normal emulsion polymerization process is followed.[16] In this way, the effective encapsulation could occur. A hydrophobic clay, compared to its intrinsic hydrophilicity, is therefore required to favor its retention within the oil phase before polymerization. This hydrophobicity will aid the entry of monomer into the intergalleries of the clay and exfoliate the clay from a stacked architecture to an individually dispersed platelet form after polymerization. Meanwhile, a complete encapsulation of the clay within a polymer shell could be achieved (Scheme 2).

Miniemulsion polymerization,[17] which is an extension of conventional emulsion polymerization by the inclusion of a small amount of a monomer-soluble, water-insoluble

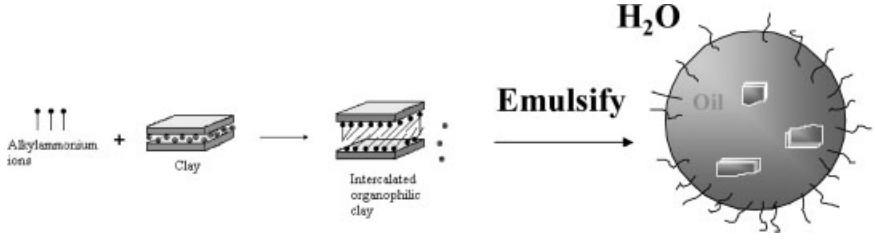

Scheme 1. Schematic demonstration of intercalation process of CTAB in the intergalleries of clay and the morphology of clay within an oil phase.

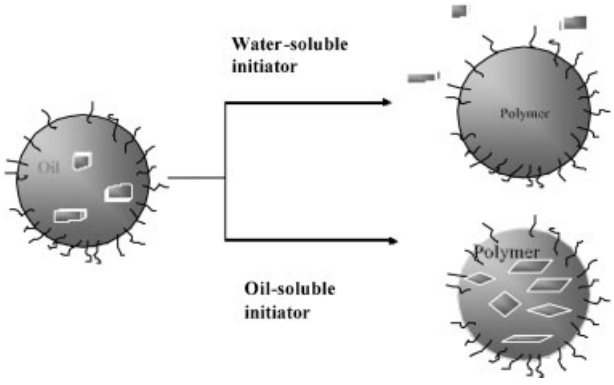

Scheme 2. Schematic demonstration of polymerization process in the presence of clay in an aqueous phase and the exfoliation of clay as embedded within a latex particle matrix.

material called costabilizer, meets most, if not all, of the above requirements for the encapsulation of a phyllosilicate layered clay. The co-stabilizer can significantly reduce the diffusional degradation (Ostwald ripening) of a monomer/water emulsion as well as reduce the monomer droplet size to within a range of 100–500 nm with shear.[16a] Hence, in a subsequent emulsion polymerization, there may be little or no micellar or homogeneous nucleation. The droplets become the primary loci of particle nucleation. To date, to the best of our knowledge, no reports exist which describe the encapsulation of phyllosilicate layered clay via this method. In this study, a miniemulsion polymerization approach was used to encapsulate laponite clay, a synthetic member of the hectorite clay family with an empirical formula of $Na^{+}_{0.7}[(Si_8Mg_{5.5}Li_{0.3})O_{20}(OH)_4]^{0.7-}$ and a charge deficiency of 0.7 per unit cell. It is comprised of six octahedral magnesium ions sandwiched between two layers of four tetrahedral silicon atoms. It has a diameter of about 300 Å and a height of about 10 Å in each layer.[18] The process parameters and influence factors for the process were examined in detail with the help of light-scattering determination of particle size, sedimentation and incineration, WXRD analysis, and TEM observations.

Experimental Part

Materials

Laponite (RD) was purchased from Southern Clay Products, Inc. It contains 59.5% SiO_2, 27.5% MgO, 0.8% Li_2O, and 2.8% Na_2O. It has a specific surface area of 370 $m^2 \cdot g^{-1}$. A cationic exchange capacity (CEC) of 7.3×10^{-4} $mol \cdot g^{-1}$ is reported.[18c,19] 2,2′-Azoisobutyronitrile (AIBN) was provided by Waco Chemicals USA, Inc. Cetyltrimethylammonium bromide (CTAB, m.p. >230 °C), myristyltrimethylammonium bromide (MTAB), octadecyltrimethylammonium bromide (OTAB), polyoxyethylene (40) isooctylphenyl ether (TX-405, chemical formula: $(4\text{-}(C_8H_{17})C_6H_4(OCH_2CH_2)_{40}OH$, 70% solution in water), cetyl alcohol (CA, 99%), and styrene (99%) were purchased from Aldrich Chemical Inc. Styrene was first washed with 5 wt.-% NaOH solution, and then washed by deionized water until pH ≈ 7. The dried styrene with a 3 Å molecular sieve was distilled under reduced pressure prior to use. All other reagents were used as received.

Instrumentation

Light-scattering measurements of particle size and distribution were carried out on a Malvern Zetasizer 3000 at 25 °C with a fixed incident angle of light at 90°. Before the measurement, either miniemulsion or latex was diluted to such an extent that the number readings of photons counted per second (cps) g were in the range of 5 000 to 12 000. The diluent was an aqueous solution containing TX-405 in the same concentration as its mother liquor to reduce the dilution effect on droplet size.[16b] The morphology of the latex particles was observed on a JEOL 100C transmission electron microscope (TEM) at an accelerating voltage of 100 kV and beam current of 70 μA. The samples were prepared by casting a drop of diluted latex solution (with the same dilution procedure as described above) onto a 200-mesh copper grid covered with carbon film and were dried at room temperature overnight. Sedimentation of either miniemulsion or latex was conducted in a Beckman 20 centrifuge at 15 000 rpm for 30 min at room temperature. The incineration experiments were carried out in an Isotemp Programmable Forced-Draft furnace (Fisher Scientific Inc.) at 525 °C for 1 h. The weight of the ash after incineration was taken as the weight of clay, after subtracting the water adsorption of ca. 3.5 wt.-%. WXRD patterns were recorded on a PW 1800 x-ray diffractometer (Philips, USA) using Cu K_α ray ($\lambda = 1.54056$ Å) as the radiation source. A step size of 0.01° and a scan step time of 0.5 s were adopted. The d(001)-spacing of the clay is calculated using the Bragg equation:

$$d = \lambda / 2 \sin \theta \quad (1)$$

where λ is the incident wavelength (1.54056 Å), and θ is the diffraction angle.[20]

The homogenization was conducted by ultrasonification on a W-385 sonicator (Heat System-Ultrasonics, Inc., USA) with samples being cooled by an ice bath, with 1 s of cycle time, 70% of duty cycle, and an output of the microtip at 5.

Basic Recipe

The basic recipe is tabulated in Table 1 except when specifically noted.

Table 1. Basic recipe.

Mixtures	Component	Amount added	Percentage in total	Percentage to monomer
		g	wt.-%	wt.-%
Mixture **A**	Styrene	6	18.0	100
	Laponite	0.25	0.75	4.2
	CTAB	0.25	0.75	4.2
	CA	0.6	1.8	10
	AIBN	0.15	0.45	2.5
Mixture **B**	TX-405	0.5	1.5	8.4
	D.I. Water	25	76	417

Preparation of the Miniemulsion

A typical procedure is as follows: the components according to the basic recipe for mixtures **A** and **B** were charged respectively into two separate glass vials (ca. 15 cm in height and ca. 2 cm in inner diameter) with a magnetic bar. **B** was prepared with simple magnetic stirring at 25 °C for 10 min, then cooled with an ice bath. After vigorous stirring for 1 h at 25 °C, **A** was cooled in an ice bath for another 10 min. Ultrasonification was followed immediately by putting the microtip beneath the surface of **A** to further disintegrate the agglomerates in the clay. Then, **A** and **B** were mixed with vigorous mechanical stirring with a downward three-blade flat stirrer in a glass beaker and agitated at ca. 1 000 rpm for 10 min. The miniemulsion prepared in this way was further homogenized with the sonicator in an ice bath for another 2 min.[13a,21] After another 10 min stirring at room temperature, this mixture was then ready for either property characterization of the miniemulsion or for subsequent polymerization.

Polymerization

The as-prepared miniemulsion was first degassed by bubbling with pure N_2 for 30 min under electromagnetic stirring (ca. 1 000 rpm) in the glass vial. Then, the temperature was raised to 65 ± 2 °C. The polymerization was conducted at this temperature for more than 4 h under continuous stirring and terminated by dropping two drops of 1% hydroquinone solution into the system. A milk-like stable miniemulsion latex was obtained under favored conditions.

Stability Observation

The stability or creaming of both miniemulsion and latex was evaluated by sedimentation tests of using static and dynamic methods. In static observation, the amount of precipitate or the height of the creaming line was recorded, if there was any, after 72 h. −, ±, and + denote poor (large amount of precipitate either at the bottom or in suspended form), fairly good (detectable amount of precipitate), and good (no precipitate and an undetectable creaming line), respectively. For dynamic observations, the sample was poured into a centrifuge tube and centrifuged at a constant speed of 15 000 rpm for 30 min. The dry weight of the precipitate at the bottom of the tube was collected and incinerated as described above.

Results and Discussion

Stability of Miniemulsions

Cationic Surfactant CTAB

To examine the effectiveness of surface modification of the clay via a cationic ion exchange method,[22] a set of experiments were conducted separately. First, the monomer phase containing laponite clay and other additives (**A**) was mechanically mixed with an aqueous phase (**B**) and left standing free on a table for 72 h. A creaming line could be observed; upon it was the oil phase, and the aqueous phase was right below this line. The two layers were separated using a separating funnel, and the distribution of clay in both phases was determined by measuring the ash weight after incineration. As depicted in Table 2, more than 88 wt.-% of clay was found within the monomer phase for the sample containing modified clay. In contrast, however, less than 10 wt.-% of clay could be detected in the monomer phase for the sample containing unmodified clay, leaving most of the clay in the aqueous phase. This clearly indicated that the clay modified with CTAB remained primarily in the oil phase under mechanical shear.

As shown in Figure 1, more than 70% of the clay was precipitated out after polymerization in the absence of CTAB. However, the precipitate was remarkably reduced to an undetectable amount for the sample containing no CTAB. Along with the introduction of CTAB, this tendency began to level off when the CTAB content exceeded 1.5 wt.-%.

Along with the variation in the content of CTAB, as disclosed in Figure 1, there were no remarkable changes in particle size before polymerization, with a fluctuation between 200 and 160 nm. The abnormally low size in the first entry in Figure 1 could be attributed to the net miniemulsion droplet size when all large particles were precipitated out with clay in the absence of CTAB.

Nonionic Surfactant TX-405

The change of particle size along with the change of TX-405 concentration is plotted in Figure 2. In contrast to the

Table 2. Distribution of laponite clay between oil and aqueous phase at TX-405 = 2.0 g. The samples collected from oil and aqueous phases were first dried at 140 °C for 3 h, and then incinerated at 525 °C for 1 h.

System	With CTAB			Without CTAB		
	Added	Measured	Percentage in fed clay	Added	Measured	Percentage in fed clay
	g	g	wt.-%	g	g	wt.-%
Oil phase	0.25	0.221	88.3	0.25	0.020	8.1
Aqueous phase	0	0.026	10.4	0	0.224	89.7

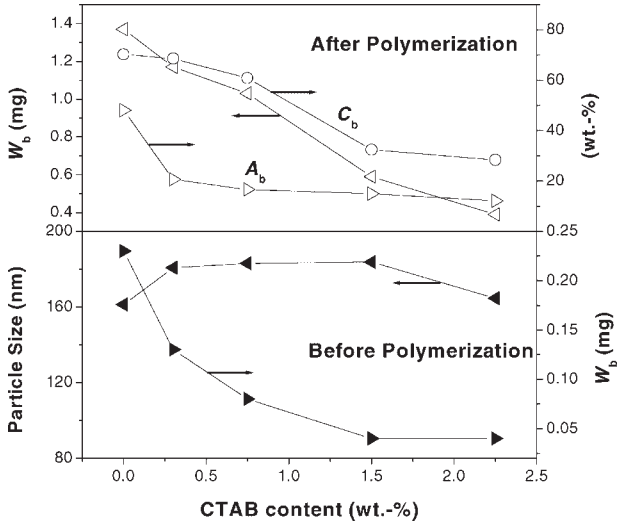

Figure 1. Relationship between CTAB content (wt.-%) and properties. Filled triangles: before polymerization; empty triangles and circle: after polymerization. The stability sequences for the above five CTAB contents (from low to high) were −, ±, +, +, and +, respectively. W_b denotes the dry weight (g) of precipitates obtained at the bottom of the centrifuge tube after sedimentation for either emulsion or latex samples. A_b denotes the weight of clay as obtained in incineration divided by the total weight of W_b multiplied by 100% (wt.-%). C_b denotes the weight of clay obtained in incineration derived from W_b divided by the total weight of clay fed, then multiplied by 100% (wt.-%). All of these parameters have been defined in the same way throughout.

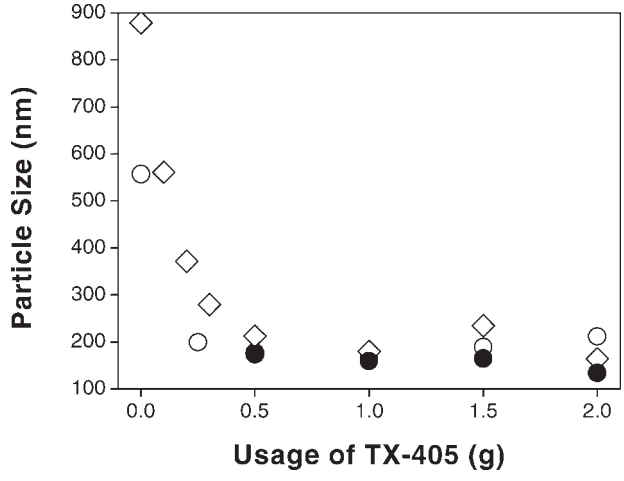

Figure 2. Relationship between particle size and TX-405 usage in the aqueous phase. Empty circle and rectangle: before polymerization; filled circle: after polymerization. ◇: CTAB = 0.25 g; ○: CTAB = 0.5 g; ●: CTAB = 0.25 g.

above observations, the droplet size for samples containing no or low usage of TX-405 before polymerization was 1 μm, about five times higher than that of the sample containing no CTAB. With the increase of TX-405 concentration in the basic recipe, the average particle size of oil droplets fell dramatically to the range of those obtained above (ca. 200 nm) and began to level off. When the usage of TX-405 was higher than 0.5 g (≈0.014 M in the aqueous phase), the stability of the system was markedly improved. This is in good agreement with the results obtained by Özdeğer et al. for a similar system with general emulsion polymerization taking account of the partitioning of TX-405 in the styrene phase.[23] It was interesting to note that the particle size before or after polymerization was basically within the same range, a result consistent with those reported in the literature.[24] It was evident that a real miniemulsion process had been accomplished. In contrast, in the absence of TX-405, the miniemulsion system was unstable. TX-405 and CTAB work in a concerted manner to stabilize the system.

Costabilizer

A prominent characteristic of the miniemulsion polymerization process, in contrast to conventional emulsion or microemulsion polymerization, has been the introduction of a third component or so-called costabilizer into the system, such as hexadecane or 1-hexadecanol. The costabilizer plays a role in retarding the diffusion of monomers from smaller to larger droplets.[13a,21,25] Cetyl alcohol, or CA, was used as costabilizer in this study. When the content of CA was changed from 0 wt.-% to 0.6 wt.-%, as shown in Table 3, the droplet size was dramatically reduced from ca. 1.1 μm to ca. 270 nm. Meanwhile, the amount of clay precipitated out was remarkably reduced. After the content of CA exceeded 1.8 wt.-% in the recipe, the particle size vs. CA content profile exhibited no remarkable fluctuation, and a stable system could be observed.

The change in the amount of clay precipitated out from the miniemulsion system also supported the above observation. As listed in Table 3, 4.4 g of precipitate containing 5.6 wt.-% of clay was detected in the absence of CA. This means that almost 100% of the fed clay (0.25 g) had been precipitated out instead of being included within the latex particles after polymerization. In other words, the system without the costabilizer CA was unstable. However, at 1.8 wt.-% of CA, only ca. 15% of fed clay could be detected in the precipitate. The function of CA in this study can thus be deduced as being a stabilizer for the miniemulsion system and possibly prohibits coalescence and coagulation between the particles.

Chain Length of the Cationic Surfactants

As illustrated in Table 4, the length of the alkyl chain (carbon numbers on the aliphatic chain) of the cationic surfactant can influence the stability of the miniemulsion system. This was demonstrated by the amount of clay precipitated out before or after polymerization. For example, in a system containing MTAB which had a shorter alkyl chain with 14 carbon atoms, a larger W_b value (0.23 g) and a bimodal particle size distribution were obtained. Nevertheless, in systems containing CTAB and OTAB which have 16 and 18 carbon atoms on the aliphatic chains respectively,

Table 3. Particle size dependence on the content of costabilizer (CA) and the stability of the miniemulsions. TX-405 = 0.3 g (0.8 wt.-%) in basic recipe.

Entry	CA content/wt.-%	0.0	0.6	1.2	1.8
Before polymerization	Particle size/nm	1073.9	279.2	267.2	261.6
	Polydispersity[a)]	0.82	0.78	0.25	0.54
	Stability	−	±	+	+
After polymerization	W_i[b)]/g	4.4	4.3	−	0.3
	A_i[c)]/wt.-%	5.6	4.5	−	12.2
	C_i[d)]/wt.-%	98.5	77.3	−	14.8
	Stability	−	±	N/A	+

[a)] Particle distribution by dynamic light-scattering measurement.
[b)] W_i refers to the dry weight (g) of precipitates obtained at the bottom of sample vial after 72 h free-standing for latex.
[c)] A_i refers to the weight of clay as obtained in incineration divided by the total weight of W_i multiplied by 100% (wt.-%).
[d)] C_i refers to the weight of clay as obtained in incineration derived from W_i divided by the total weight of clay fed, then multiplied by 100% (wt.-%). W_i, A_i, and C_i have been defined the same throughout.

only a trace amount of precipitated clay could be detected (W_b was equal to 0.004 g and 0.01 g respectively). Meanwhile, the distributions of particle size were both monomodal and consistent with the results reported in the literature.[23,25a]

Instrumentation

WXRD

Spectral information on the platelet structure of the clay in the systems studied can be obtained by the WXRD analysis.[4,26] As depicted in Figure 3, while the WXRD pattern of pristine laponite only exhibited one diffraction peak (**A**) at 2θ ca. 7.0° and with a *d*(001)-spacing of ca. 13 Å,[27] the diffraction profile of the clay dispersed in the monomer phase in the absence of CTAB was centered at 2θ ca. 4.8° with a *d*-spacing of ca. 18 Å (**B**). Nevertheless, no prominent changes could be observed after polymerization (**C**). In the presence of CTAB, the WXRD profile of the clay exhibited a broad peak centered at 2θ ca. 4.6° (**D**) and a *d*(001)-spacing ca. 19 Å. This indicates a range of spacing distance distribution of the clay being inserted by CTAB, as reported for other systems.[19,28] After polymerization,

Table 4. Influence of chain length of cationic surfactants on particle size and miniemulsion stability. The reactions were carried out following the basic recipe and typical procedures as described in the text.

Surfactant type	MTAB	CTAB	OTAB
W_i/g	Trace	Trace	Trace
W_b[a)]/g	0.23	0.004	0.01
Particle size/nm	257.7	211.6	197.0
Polydispersity	0.41	0.23	0.20
Peak shape (distribution)	Bi-	Mono-	Mono-
Stability	±	+	+

[a)] W_b refers to the dry weight (g) of precipitates obtained at the bottom of the centrifuge tube after sedimentation for the miniemulsion samples, with the same definition throughout.

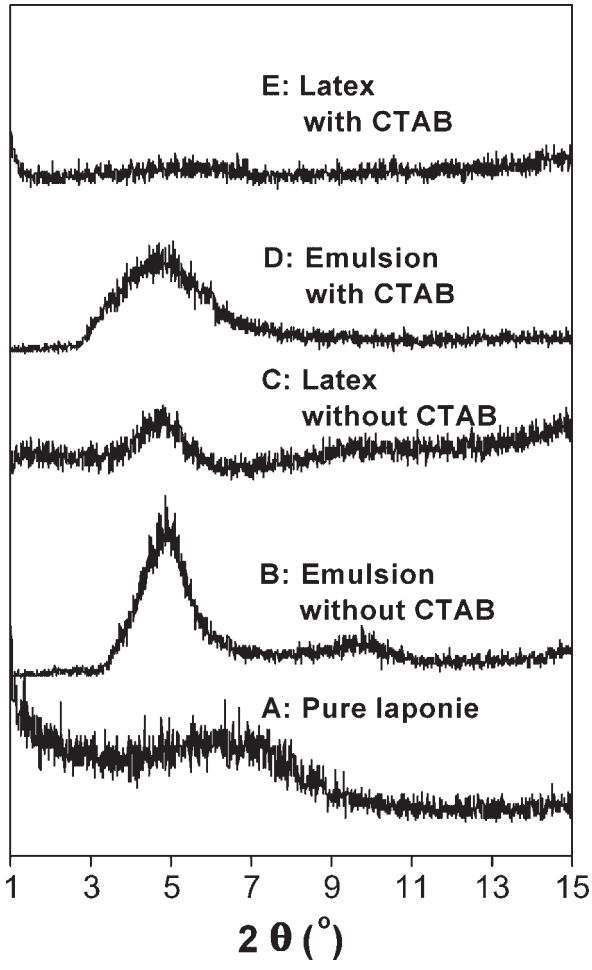

Figure 3. WXRD pattern of **A**: pristine laponite clay; **B**: precipitate collected from sample without CTAB before polymerization (clay content: 90 wt.-%); **C**: precipitate collected from sample without CTAB after polymerization (clay content: 6.0 wt.-%); **D**: precipitate collected from sample with CTAB before polymerization (clay content: 90 wt.-%); and **E**: precipitate collected from sample with CTAB after polymerization (clay content: 7.8 wt.-%).

however, no apparent diffraction peaks, as depicted on curve **E**, could be detected in the whole range, suggesting a fully exfoliated structure of the laponite clay.[4,5,29] These results were highly consistent with those above. Generally speaking, it was apparent that a dramatic difference of WXRD profiles existed between the samples with or without CTAB. It was thus deduced that the insertion of CTAB into the intergalleries allowed not only the pertinent hydrophobicity, helping confine the clay inclusion within the monomer droplets during the droplet formation prior to polymerization, but also aided the continuous monomer entry in the subsequent polymerization. In this way, the exfoliation of the clay could be fostered and finally achieved.

TEM

The TEM technique can reveal direct morphology or even the interior structure of a latex particle if it is properly positioned. As disclosed in Figure 4 **A**, the latex particles, in the absence of clay, were spherical in shape with an average particle size of ca. 60 nm. However, for the sample containing clay, the morphology and size of the latex particles were different (Figure 4 **B**). It was found that irregular coarse-edged spheres and uneven density within the confined boundary of each particle could be observed. In addition, the particle size was ca. 200 nm, consistent with the results obtained from light-scattering measurements as mentioned above, but much larger (2–3 times) than those containing no clay. Taking account of the sophisticated formation of laponite clay as well as the interference of the polymer shell layer,[30] the morphology observed was not difficult to understand. A closer examination of the morphology of one latex particle containing laponite clay is disclosed in Figure 5; a number of randomly distributed nanoparticles with diameters at ca. 30 nm could be observed in and on the sphere. These particles could be reasonably deduced to be the existing clay, in terms of the disk-like morphology of the laponite clay introduced.[18]

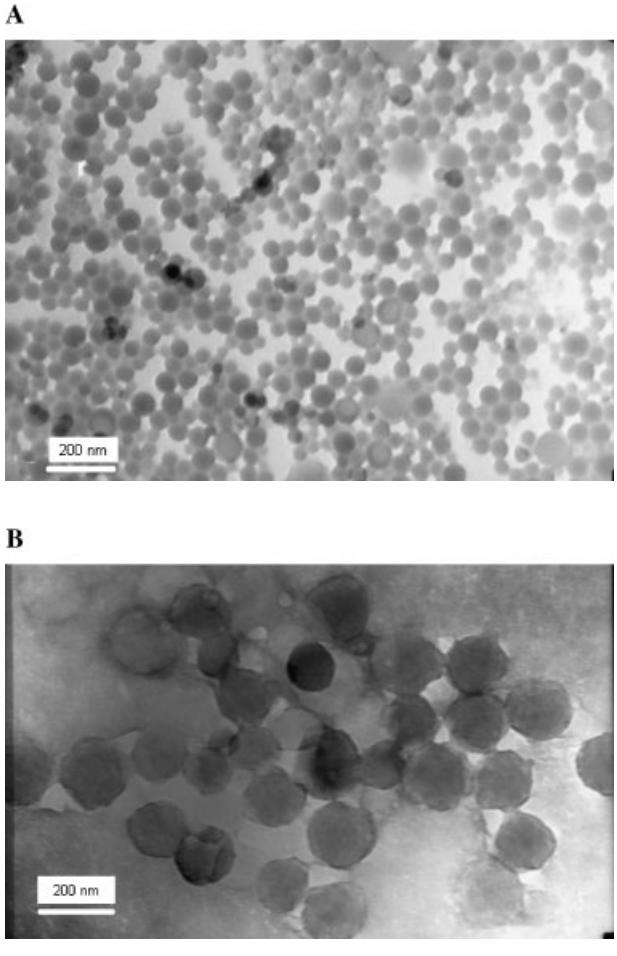

Figure 4. TEM photographs of **A**: latex particles without clay and **B**: latex particles with clay.

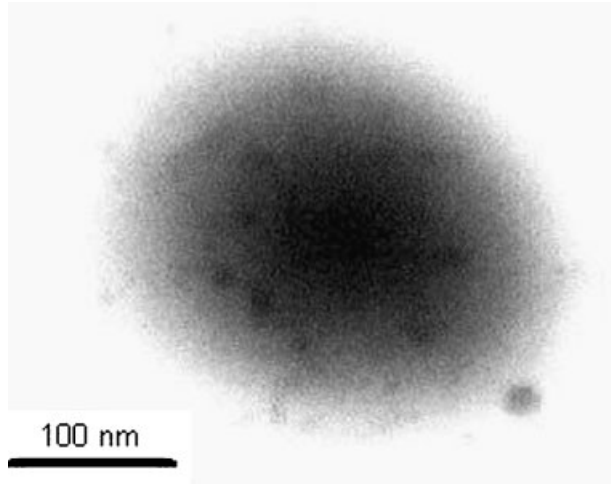

Figure 5. TEM observation of one latex particle's morphology. Scale bar: 100 nm.

Conclusions

A novel polystyrene-encapsulated laponite hybrid system in the form of a water dispersion was developed with up to ca. 5 wt.-% of clay loading via a miniemulsion polymerization approach. The polymer/nanoclay hybrid obtained in this way was macroscopically homogeneous and stable, with clay being included within the polymer latex particles with a fully exfoliated structure. Results showed that the stabilizer and costabilizer, ultrasonification time and other process parameters played a collaborative role in stabilizing the miniemulsion. The role of cationic surfactant CTAB introduced in the monomer phase was unique. In addition to its costabilization effect as an emulsifier, it allowed the hydrophobic clay as an intercalant in the intergallery space of the clay, and helped the clay to be retained within the oil phase during subsequent processes. The size of latex particles impregnated with clay preserved the identity before and after polymerization and was in the range of 180

to 200 nm according to both TEM observation and light-scattering measurements. WXRD results showed that the laponite clay had been fully exfoliated in the presence of CTAB after polymerization. The sedimentation tests demonstrated that the method was effective for characterizing the apparent stability of both emulsion and latex as a supplementary tool when used in conjunction with other instrumentation methods.

Acknowledgement: The support of a grant from the *NSF* (Grant Number CTS-0244371) is gratefully acknowledged. The authors appreciate the help and assistance of Mr. *P. Jorge*, Mr. *A. Ball*, and Dr. *Z. Hu* during the research. The assistance of Mrs. *B. Yolande* and Mr. *J. Cagle* in the School of Materials Science and Engineering at the Georgia Institute of Technology is greatly appreciated.

[1] [1a] "*Polymer-Clay Nanocomposites*", T. J. Pinnavaia, G. W. Beall, Eds., John Wiley & Sons, New York 2000, p. 1; [1b] D. W. Bruce, D. O'Hare, "*Inorganic Materials*", 2nd edition, John Wiley & Sons, New York 1996; [1c] B. K. G. Theng, "*Formation and Properties of Clay-Polymer Complexes*", Elsevier, New York 1997. [1d] H. H. Murray, *Appl. Clay. Sci.* **2000**, *17*, 207.

[2] [2a] A. Okada, A. Usuki, T. Kurauchi, O. Kamigaito, in: "*Hybrid Organic-Inorganic Composites*", J. E. Mark, C. Y.-C. Lee, P. A. Bianconi, Eds., American Chemical Society, Washington DC 1995, p. 55; [2b] A. Usuki, M. Kawasumi, Y. Kojima, A. Okada, T. Kurauchi, O. Kamigaito, *J. Mater. Res.* **1993**, *8*, 1174; [2c] A. Usuki, Y. Kojima, M. Kawasumi, A. Okada, Y. Fukushima, T. Kurauchi, O. Kamigaito, *J. Mater. Res.* **1993**, *8*, 1179; [2d] Y. Kojima, A. Usuki, M. Kawasumi, A. Okakda, Y. Fukushima, T. Kurauchi, O. Kamigaito, *J. Mater. Res.* **1993**, *8*, 1185.

[3] [3a] E. P. Giannellis, *Adv. Mater.* **1996**, *8*, 29; [3b] C. Nah, H. J. Ryu, W. D. Kim, S. S. Choi, *Polym. Adv. Technol.* **2002**, *13*, 649.

[4] L. Liang, J. Liu, X. Gong, *Langmuir* **2000**, *16*, 9895.

[5] J.-M. Yeh, S.-J. Liou, C.-Y. Lin, C.-Y. Cheng, Y.-W. Chang, *Chem. Mater.* **2002**, *14*, 154.

[6] K. Yano, A. Usuki, T. Kurauchi, O. Kamigaito, *J. Polym. Sci., Part A: Polym. Chem.* **1993**, *31*, 2493.

[7] R. W. Grimshaw, in: "*The Chemistry and Physics of Clays and Advanced Ceramic Materials*", TechBooks, Fairfax VA 1971, p. 124.

[8] M. V. Smalley, *Langmuir* **1994**, *10*, 2884.

[9] X. Huang, W. J. Brittain, *Macromolecules* **2001**, *34*, 3255.

[10] [10a] US 5,766,817 (1998), Xerox Corporation, invs.: C.-M. Cheng, M.-H. Fu; [10b] US 5,215,847 (1993), Xerox Corporation, invs.: R. Patel, H. Mahabadi, T. Bluhm, S. Gardner.

[11] J. W. Kim, H. J. Choi, M. S. Jhon, *Macromol. Symp.* **2000**, *155*, 229.

[12] B. zu Putlitz, K. Landfester, H. Fischer, M. Antonietti, *Adv. Mater.* **2001**, *13*, 500.

[13] [13a] B. Erdem, E. D. Sudol, V. L. Dimonie, M. S. El-Aasser, *J. Polym. Sci., Part A: Polym. Chem.* **2000**, *38*, 4419; [13b] N. Bechthold, F. Tiarks, M. Willert, K. Landfester, M. Antonietti, *Macromol. Symp.* **2000**, *151*, 549.

[14] C. Caris, L. Elven, A. van Herk, A. German, *Br. Polym. J.* **1988**, *21*, 133.

[15] F. Tiarks, K. Landerfester, M. Antonietti, *Macromol. Chem. Phys.* **2001**, *202*, 51.

[16] [16a] J. L. Reimer, F. Schork, *J. Ind. Eng. Chem. Res.* **1997**, *36*, 1085; [16b] C. S. Chern, T. J. Chen, Y. C. Liou, *Polymer* **1998**, *39*, 3767.

[17] J. Ugelstad, M. S. El-Aasser, J. W. Vanderhoff, *J. Polym. Sci., Polym. Lett. Ed.* **1973**, *11*, 503.

[18] [18a] M. Kroon, W. Vos, G. H. Wegdam, *Phys. Rev. E* **1998**, *57*, 1962; [18b] A. Mourchid, A. Delville, J. Lambard, E. Lécolier, P. Levitz, *Langmuir* **1995**, *11*, 1942, and references therein; [18c] J. D. F . Ramsey, *J. Colloid. Interface. Sci.* **1986**, *109*, 441; [18d] D. Bonn, H. Kellay, H. Tanaka, G. Wegdam, J. Meunier, *Langmuir* **1999**, *15*, 7534; [18e] J. O. Fossum, *Physica A* **1999**, *270*, 270.

[19] D. Kubies, R. Jérôme, J. Grandjean, *Langmuir* **2002**, *18*, 6159.

[20] [20a] Q. Sun, K. Xu, H. Peng, R. Zheng, M. Haussler, B. Z. Tang, *Macromolecules* **2003**, *36*, 2309; [20b] Q. Sun, J. W. Y. Lam, K. Xu, H. Xu, J. A. K. Cha, P. C. L. Wong, G. Wen, X. Zhang, X. Jing, F. Wang, B. Z. Tang, *Chem. Mater.* **2000**, *12*, 2617.

[21] K. Landfester, *Adv. Mater.* **2001**, *13*, 765.

[22] K. Esumi, Y. Takeda, M. Goino, K. Ishiduki, Y. Koide, *Langmuir* **1997**, *13*, 2585.

[23] [23a] E. Özdeğer, E. D. Sudol, M. S. El-Aasser, A. Klein, *J. Polym. Sci., Part A: Polym. Chem.* **1997**, *35*, 3813; [23b] E. Özdeğer, E. D. Sudol, M. S. El-Aasser, A. Klein, *J. Polym. Sci., Part A: Polym. Chem.* **1997**, *35*, 3837.

[24] K. Landfester, N. Bechthold, S. Förster, M. Antonietti, *Macromol. Rapid Commun.* **1999**, *20*, 81.

[25] [25a] P. J. B. Blythe, E. D. Sudol, M. S. El-Aasser, *Macromol. Symp.* **2000**, *150*, 179, and references therein; [25b] E. D. Sudol, M. S. El-Aasser, in "*Emulsion Polymerization and Emulsion Polymers*", P. A. Lovell, M. S. El-Aasser, Eds., J. Wiley & Sons, New York 1997, p. 699.

[26] T. Yui, H. Yoshida, H. Tachibana, D. A. Tryk, H. Inoue, *Langmuir* **2002**, *18*, 891.

[27] M. M. Doeff, J. S. Reed, *Solid State Ionics* **1998**, *113–115*, 109.

[28] I. Grillo, P. Levitz, Th. Zemb, *Langmuir* **2000**, *16*, 4830.

[29] [29a] X. Fu, S. Qutubuddin, *Mater. Lett.* **2000**, *42*, 12; [29b] X. Huang, S. Lewis, W. J. Britain, *Macromolecules* **2000**, *33*, 2000; [29c] H. Shi, T. Lan, T. Pinnavaia, *J. Chem. Mater.* **1996**, *8*, 1584; [29d] M. H. Choi, I. J. Chung, J. D. Lee, *Chem. Mater.* **2000**, *12*, 2977; [29e] D. Kong, C. E. Park, *Chem. Mater.* **2003**, *15*, 419.

[30] [30a] M. Kroon, W. L. Vos, G. H. Wegdam, *Phys. Rev. E* **1998**, *57*, 1962; [30b] D. Bonn, H. Kellay, H. Tanaka, G. Wegdam, J. Meunier, *Langmuir* **1999**, *15*, 7534.

